

RLCorrector: Reinforced Proofreading for Connectomics Image Segmentation

Khoa Tuan Nguyen, Ganghee Jang, and Won-ki Jeong

Korea University, Seoul, Republic of Korea
{ntkhoa, jnggh, wkjeong}@korea.ac.kr

Abstract. The segmentation of nanoscale electron microscopy (EM) images is crucial but challenging in connectomics. Recent advances in deep learning have demonstrated the significant potential of automatic segmentation for tera-scale EM images. However, none of the existing segmentation methods are error-free, and they require proofreading, which is typically implemented as an interactive, semi-automatic process via manual intervention. Herein, we propose a fully automatic proofreading method based on reinforcement learning. The main idea is to model the human decision process in proofreading using a reinforcement agent to achieve fully automatic proofreading. We systematically design the proposed system by combining multiple reinforcement learning agents in a hierarchical manner, where each agent focuses only on a specific task while preserving dependency between agents. Furthermore, we also demonstrate that the episodic task setting of reinforcement learning can efficiently manage a combination of merge and split errors concurrently presented in the input. We demonstrate the efficacy of the proposed system by comparing it with state-of-the-art proofreading methods using various testing examples.

Keywords: Reinforcement Learning · Proofreading · Connectomics

1 Introduction

Connectomics is an advanced research field for investigating cellular-level neural connections in the brain [6]. In this research field, nanoscale electron microscopy (EM) images are typically used to resolve tiny neuronal structures (e.g., dendritic spine necks and synapses) of only tens of nanometers [11]. A conventional connectome analysis workflow using EM images comprises data acquisition (slicing the tissue into thin serial sections and imaging), image processing (segmentation of neuronal structures in the image), and analysis (interpretation of the segmentation result). Because the raw data size of EM serial sections of a small tissue sample can easily reach hundreds of terabytes, the development of high-throughput and automatic image processing algorithms has been actively studied in cellular-level connectomics research [11].

Recent advances in deep learning have indicated the significant potential of the high-throughput, automatic segmentation of connectome images. The most

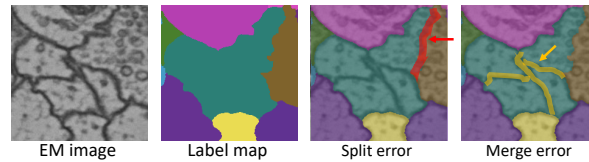


Fig. 1. Example of segmentation errors for proofreading. Merge error occurs when more than two independent objects are incorrectly merged and assigned the same label. Split error occurs when single object is incorrectly split into multiple segments and assigned different labels.

of the related methods are based on pixel-level classification using convolutional neural networks (CNNs) and instance clustering [17,4,14]. However, all existing methods are not perfect and prone to errors, particularly when applied to real data, which requires manual proofreading by humans. Existing proofreading methods are primarily based on the interactive manual correction of either merge or split errors (see Figure 1) using an intuitive user interface and visualization [9,12]. Even with the support of such interactive tools, manual proofreading is a time-consuming and labor-intensive task, resulting in a bottleneck in the connectome analysis workflow. Recently, Haehn *et al.* [8] significantly simplified the manual proofreading process using a suggestion system; however, the method still requires human intervention, and the accuracy of the proofreading depends primarily on the performance of the CNN classifier.

The main motivation of this study stems from the observation that reinforcement learning (RL) can mimic the human decision process. Since Mnih *et al.* [16] pertaining to RL using deep neural networks, many human-level decision-making tasks have been solved using RL. Originally, RL algorithms have been applied to solve problems whose settings can be easily transformed into a series of decisions, called the Markov decision process (MDP) [19], where the RL agent makes a decision based only on the current state and input signal. However, conventional image processing tasks typically do not involve decisions over time. Therefore, the area adapts RL relatively more slowly than other domains. Recently, several notable studies have been performed to solve image-processing problems using RL. For example, PixelRL [7] modeled an image processing task as a series of per-pixel filters determined by RL agents. Uz Kent *et al.* [20] proposed an image classification problem to perform patch selection using RL, in which a human’s ability to identify an object from a few notable details is mimicked. Araslanov *et al.* [2] formulated an instance segmentation problem into a sequential object detection and segmentation problem, which maps to the decision-making process in RL. Similarly, we believe that the proofreading problem can be formulated as a series of decision-making (i.e., identifying the erroneous location, identifying the error type, and deciding to continue or stop) that fits well with the RL formulation.

Hence, we propose a novel RL-based automatic proofreading method for connectomics image segmentation, which is inspired by the human decision pro-

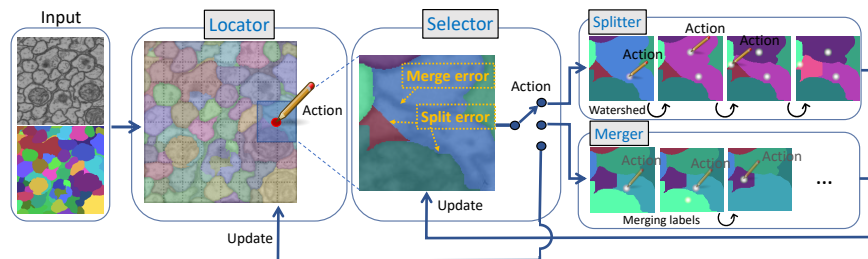


Fig. 2. Overview of the proposed RL proofreading system. Human decision flow is mapped to agent actions. Updates are from individual correctors and used for decision making at next time step.

cess. We identified the basic units of the human decision process as subtasks in the proofreading problem, where each of them can be modeled using an RL agent. Subsequently, the system can be constructed in a bottom-up approach, which naturally forms a nested loop structure. Another benefit of using RL in proofreading is that learning can be performed by exploring the action space. The proposed system iteratively selects either merge or split error correctors to achieve optimal proofreading results. This episodic problem setting allows the RL agent to learn the optimal operation ordering without using the ground truth ordering and to fix multiple errors concurrently presented in a single image efficiently. This is the major difference from the conventional CNN-based method (e.g., Haehn *et al.* [8]), where all possible errors should be computed and sorted explicitly to obtain the optimal order of error correction. To the best of our knowledge, this is the first RL-based proofreading system that operates fully automatically without human intervention.

2 Method

2.1 System overview

Similar to the human proofreading process, our automatic proofreading process comprises subtasks in series. A proofreading process begins with identifying a patch with errors (the locator), selecting an error fixing method (the selector), and performing error correction (the merger and splitter). As depicted in Figure 2, each component (subtask) is implemented using an RL agent, where the decision made by an agent is used as the input to the next agent.

The locator’s task is to identify a patch with errors, and this is repeated until no erroneous patches are left. This series of actions form an episode. The error location is selected coarsely by a grid point chosen by the locator agent. Once a patch is selected, the selector selects an error correction method. A patch can include a combination of errors. Therefore, the selector can yield series of decisions until no further errors are identified. Furthermore, the selected merger or splitter agent conducts a series of decisions to perform error-correcting

operations. Once a locator agent selects a patch, the locator environment copies and forwards the corresponding part of the label map to the selector, which serves as the initial state for the selector. When the selector terminates its episode, the label map should be updated on the label map of the locator. In fact, the selector does not perform error correction by itself but generates the order of the application of mergers and splitters. The updates for the label map updates originates from the merger or splitter.

During training, the environment should present a reward to encourage each agent to perform learning towards the optimal decision. We employed the circuit reconstruction from electron microscopy images (CREMI) score [5] from the MICCAI 2016 challenge as a decision metric for rewards. The score is based on the geometric mean of variation of information [13] and adapted rand error [3] between segmentation and the ground truth. With lesser difference from the ground truth, the score becomes lower, which implies less errors. Additionally, because we can judge when to terminate an episode during training time with CREMI score, a stop signal can be trained. The stop signal is an addition to the action set of each agent. While evaluating the performance using our test set, the environment can also perform termination of an episode when there are no notable changes on the label map over time. The stop signals of the agents are generally part of the entire terminal conditions. As in [18,1], setting the maximum size of each episode is a general approach. The additional ability to terminate is expected to render our algorithm more stable and safer.

2.2 Details of RL Agents

We used the asynchronous advantage actor–critic method [15] based on a CNN for the base architecture of the RL agent as shown in Figure 3. The actor learns a policy directly while the critic learns a state value. Consequently, the algorithm achieves a lower variance and faster learning. The function approximator for the actor and critic contains one convolutional layer (orange arrow) followed by five residual units (green arrows) of full pre-activation [10]. A fully connected layer is added after flattening (violet arrow). The input vector shape is $128 \times 128 \times 3$ including an EM image (scaled down from 512×512), a point map, and a label map. The large blue box represents an output feature vector from a layer or residual unit. The small blue box indicates a logit function. For training efficiency, the actor and critic share the neural network except for the fully connected layer. The actor’s output vector size is the number of actions, whereas the critic’s value function has one logit.

The locator. The locator is selecting a sub-region (i.e., patch) with errors from an input image with the label map. We used a 7×7 two-dimensional (2D) grid to define a finite action space with 49 locations, where the selected point collects four adjacent squares with dashed lines (see Figure 2). Furthermore, we used a *point map*, which is used to encourage the selection of different patches with every time step by monitoring the previously selected points as a weighed map. We generated the point map by applying a Gaussian kernel to provide a decent amount of field-of-view to the CNN used by the agent. As for the reward, we

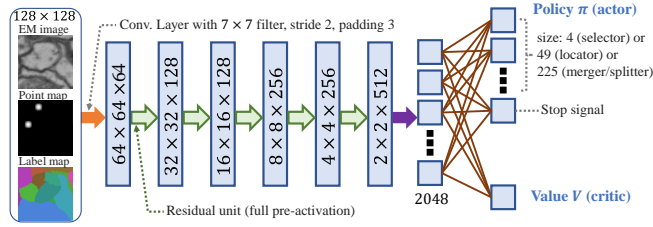


Fig. 3. Neural network architecture of RL agent. Point map is omitted when using selector agent. Output vector size of actor varies with agents.

should consider the quality of merge and split error correction to encourage the selection of the patches with errors, and we measured the quality using a CREMI score. When an action c_t is performed at time step t , the selected patch P_{c_t} and its label map L_t are forwarded to the selector. When $P_{c_t} \in E_t$ (the set of error patches), a positive reward of 1 is received. R_{diff} is added to promote the locator to select the patch with errors (such that the CREMI score of the resulting label map L_{t+1} returned from the selector is reduced). The entire reward function for the locator is shown in Equation 1.

$$R_{t+1} = \begin{cases} 1 + R_{diff} & \text{if } CREMI(L_{t+1}) < CREMI(L_t) \text{ and } P_{c_t} \in E_t \\ 0 & \text{if CREMI score has been equal to 0 once,} \\ & \text{or the episode is terminated} \\ -1 & \text{otherwise} \end{cases} \quad (1)$$

$$R_{diff} = \frac{CREMI(L_t) - CREMI(L_{t+1})}{CREMI(L_t)} \quad (2)$$

The selector. The MDP formulated by the selector is a series of selections among the merger, splitter, and stop actions. For merger and splitter actions, the agent launches a new episode to fix the corresponding errors (i.e., merge or split errors). The stop action ends the current episode made by the selector and the execution is returned to the locator. Because the action space of the selector is not defined in the 2D space, no point map exists. The input vector size to the agent is $128 \times 128 \times 2$. The reward formula is similar to that shown in Equation 1, but the positive reward conditions are different. The positive reward is for $CREMI(L_{t+1}) < CREMI(L_t)$, as no grid actions are involved. To encourage termination of an episode when necessary, we give 1 for proper terminations. We set the maximum length of a selector episode to six to encourage exploration during training (it is reduced to four during inference). If the merger and splitter are perfect, then the length of the selector’s episode can be shortened (one or two) because each agent will fix all the errors of the same type in one correction episode (merger or splitter). However, we wanted to prepare the cases of unexpected cases including more errors of the same type than six. That is another

reason why we set the maximum length of the selector bigger than 2. Figure 4 shows an example of a selector episode. Each label map under selector time step is the result of a merger or splitter episode. At $t = 1$, a wrong pair of segments are merged, but by applying another merger and a splitter episode, the errors are fixed completely. This demonstrates the manner in which selector explores the action space and solves the problem.

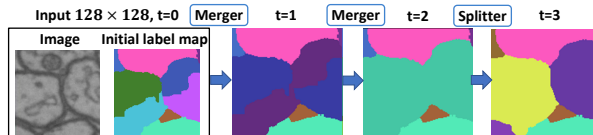


Fig. 4. Example of selector episode. Label map of each time step is from correctors. At $t = 1$, merger fails to fix merge error appropriately. To compensate, selector selects merger ($t = 2$) and splitter ($t = 3$).

The splitter. The main task of the splitter is to select a segment with a merge error (i.e., a single label is incorrectly assigned to multiple objects) in the label map and split it into multiple segments. Because the number of objects in a patch can vary, we cannot design the action space based on the object. Instead, we performed discrete sampling on a 2D space (similar to the locator) to identify the location of an object. Therefore, the agent design of the splitter is similar to that of the locator, but a finer grid space is selected, such that the total actions for the grid selection are 15×15 . For a selected grid point, the watershed algorithm is applied to separate a segment out. The point serves as a valley, and the basin grows until it reaches barriers or threshold. The filled area becomes a new segment indicated by the point. To achieve the intended operation, pre-processing is applied on the EM image, e.g., Gaussian filtering and normalization. This is repeated until no merge errors remain in the patch. The reward function of the splitter is almost identical to that of the locator, except the positive reward condition; when the segment pointed by an action belonged to the set of error segments in the patch at time t , and the CREMI score decreased over the previous time step.

The merger. The merger is identical to the splitter, except the episode settings. The merging operation requires at least one pair of neighboring segments. Therefore, we applied the merging operation once every two time steps (i.e., after selecting two grid points). An example of a single merge operation after two time steps of a merger episode is shown in Figure 5.

3 Results

3.1 Experiment settings

We used a CREMI data set [5], which comprised 125 slices of 1250×1250 . The first 92 slices were used for training, 23 for validating, and 10 for testing. The

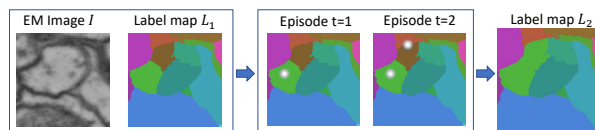


Fig. 5. Example of merger episode. Two time steps are required to select two grid points to execute a single merge operation.

error labels were created synthetically. Merge errors were generated by merging randomly selected neighboring segment labels. The watershed algorithm was used to add a new segment for a split error. We limited the maximum errors to six for the merge error, and four for the split errors in a patch to set the maximum episode size to six during training. Training was performed in the bottom-up approach. The merger and splitter were trained first, followed by the selector, and then the locator. During training, the exploration factor, ϵ was changed from 1 to 0.1. The discount factor, γ was 0.9. For the agents, we used the Adam optimizer and set the learning rate to 10^{-5} . We compared our method with an *automatic* version of Haehn’s guided proofreading [8] by letting the method fix all the errors above the given threshold. For a fair comparison, we used our agent’s backbone network for the proofreading classifier of Haehn’s to give a similar model capacity.

3.2 Performance comparisons

Table 1 shows the per-patch experiment results, where “M” represents the performance of merger algorithms (split error correction), “S” for the splitter, and “C” for the combination of two. The combination implies the ranking system for Haehn’s. We tried a static combination model for comparison with Haehn’s, where the merger and splitter are applied once in a pre-defined order. We applied the settings to three types of test set with 1000 patches. In case of the merge error test set, a good split error correction algorithm will show a marginal change because there is no split errors but a large decrease in CREMI score with a splitter (merge error corrector) and combined algorithms (which can fix merge errors). The result shows that our algorithms performed as expected.

Ours did better with the merge error set while Haehn’s did better with the split error set. However, ours outperformed with “C” due to the following. First,

	Test set	Haehn’s [8]			Ours			
		M	S	C	M	S	C(Static)	C(Selector)
Merge error	0.173	0.179	0.075	0.081	0.177	0.033	0.035	0.032
Split error	0.152	0.012	0.161	0.019	0.028	0.158	0.032	0.020
Combination	0.272	0.169	0.216	0.111	0.173	0.167	0.049	0.046

Table 1. Per-patch performance measured in the average CREMI score (lower is better). The best result for each error type is marked in bold.

ours made less errors from wrong operation. For example, a merge error corrector (splitter) should not work on split errors. As the results shown in the column of “C” in Haehn’s and C(Static) in ours), Haehn’s performance became worse in bigger margins than ours.

The results under “C(Selector)” shows results with the selector agent. The selector selects among no-correction, the merger and the splitter dynamically. On the contrary, Haehn’s method applies its error correctors in a predefined order. Our “C(Static)” case uses the same predefined order for comparison. “C(Selector)” shows the best performance overall. The selector agent helps to achieve better performance over “C(Static)” because it skips the patches with no errors without correction. Having best scores at “C” is important because a system should include the merger and splitter together. Overall, our RL agents can fix the errors well as human did and outperformed Haehn’s method in most cases we tested.

We want to point out that we applied a fix on Haehn’s method. Haehn’s splitter design sometimes ran infinitely because the error probability from fixed segments were still higher than the threshold due to incorrect error fixing (which can be prevented if human was in the loop). It is mostly due to small fragments from the watershed algorithm used in their splitter. We filtered out small fragments in order to avoid the cases. We applied this fix to every experiment shown here.

	Test set	Haehn’s	Ours		
		Sliding	Sliding(Static)	Sliding(Selector)	Locator(Selector)
Ave. score	0.138	0.156	0.078	0.054	0.049
Ex. time (min.)	N/A	88.3	24.8	19.3	7.1

Table 2. Per-image performance in the average CREMI score and execution time.

The primary benefit of using RL on the selector and locator is execution time reduction shown in Table 2. We prepared 20 EM images which are randomly cropped into 512 by 512 from the CREMI data set with 26.4% of randomly generated errors counted in patches. Errors are mixture of split and merge errors. The full RL versions (i.e., locator-selector, sliding-static, and sliding-selector) reduced the execution time by 92.0%, 78.1%, and 71.9% over Haehn’s, respectively. Note also that our locator-selector achieved better accuracy compared to sliding-selector (which is a brute-force application of the selector over the entire set of patches) using only 36.8% of running time. The running time decreases come from the reduced amount of computation by the locator (the agent selects only the erroneous patches). At the same time, the use of the reinforcement learning algorithm helped to prevent the performance loss due to the selective error correction.

4 Conclusion

Inspired by a human decision process, we introduced a novel proofreading system. We formulated each task in the proofreading process using an RL framework, and designed our system as a multi-agent system. Each task of the human proofreading process was mapped to a separate agent. By performing an action from an agent triggering the following agent, we can combine them into a system. We demonstrated that the use of an episodic setting was beneficial for improving the performance and execution time compared with other methods, and that it enabled fully automatic proofreading. One limitation of our method is that small fragments may not be managed well owing to the coarse and discrete action space. This can be addressed by employing a continuous action space. Furthermore, extension to three dimensions is another interesting direction for future investigations.

References

1. Anh, T.T., Nguyen-Tuan, K., Quan, T.M., Jeong, W.K.: Reinforced Coloring for End-to-End Instance Segmentation. arXiv:2005.07058 [cs, eess] (May 2020), <http://arxiv.org/abs/2005.07058>, arXiv: 2005.07058
2. Araslanov, N., Rothkopf, C.A., Roth, S.: Actor-critic instance segmentation. In: Proceedings of the IEEE Conference on Computer Vision and Pattern Recognition. pp. 8237–8246 (2019)
3. Arganda-Carreras, I., Turaga, S.C., Berger, D.R., Cireşan, D., Giusti, A., Gambardella, L.M., Schmidhuber, J., Laptev, D., Dwivedi, S., Buhmann, J.M., Liu, T., Seydhosseini, M., Tasdizen, T., Kamentsky, L., Burget, R., Uher, V., Tan, X., Sun, C., Pham, T.D., Bas, E., Uzunbas, M.G., Cardona, A., Schindelin, J., Seung, H.S.: Crowdsourcing the creation of image segmentation algorithms for connectomics. *Frontiers in Neuroanatomy* **9** (2015). <https://doi.org/10.3389/fnana.2015.00142>, <https://www.frontiersin.org/articles/10.3389/fnana.2015.00142/full#h3>
4. Beier, T., Pape, C., Rahaman, N., Prange, T., Berg, S., Bock, D., Cardona, A., Knott, G.W., Plaza, S.M., Scheffer, L.K., Köthe, U., Kreshuk, A., Hamprecht, F.A.: Multicut brings automated neurite segmentation closer to human performance. *Nature Methods* **14**, 101–102 (2017). <https://doi.org/10.1038/nmeth.4151>, <http://rdcu.be/oVDQ>
5. CREMI: Miccai challenge on circuit reconstruction from electron microscopy images (2016), <https://cremi.org>
6. DeWeerd, S.: How to map the brain. *Nature* **571**(7766), S6–S6 (2019)
7. Furuta, R., Inoue, N., Yamasaki, T.: PixelRL: Fully Convolutional Network With Reinforcement Learning for Image Processing. *IEEE Transactions on Multimedia* **22**(7), 1704–1719 (Jul 2020). <https://doi.org/10.1109/TMM.2019.2960636>, conference Name: IEEE Transactions on Multimedia
8. Haehn, D., Kaynig, V., Tompkin, J., Lichtman, J.W., Pfister, H.: Guided proofreading of automatic segmentations for connectomics. In: Proceedings of the IEEE Conference on Computer Vision and Pattern Recognition. pp. 9319–9328 (2018)
9. Haehn, D., Knowles-Barley, S., Roberts, M., Beyer, J., Kasthuri, N., Lichtman, J.W., Pfister, H.: Design and evaluation of interactive proofreading tools for connectomics. *IEEE transactions on visualization and computer graphics* **20**(12), 2466–2475 (2014)

10. He, K., Zhang, X., Ren, S., Sun, J.: Identity mappings in deep residual networks. In: European conference on computer vision. pp. 630–645. Springer (2016)
11. Helmstaedter, M.: Cellular-resolution connectomics: challenges of dense neural circuit reconstruction. *Nature methods* **10**(6), 501–7 (2013)
12. Knowles-Barley, S., Roberts, M., Kasthuri, N., Lee, D., Pfister, H., Lichtman, J.W.: Mojo 2.0: Connectome annotation tool. *Frontiers in Neuroinformatics* **60**, 1 (2013)
13. Meilă, M.: Comparing Clusterings by the Variation of Information. In: Schölkopf, B., Warmuth, M.K. (eds.) *Learning Theory and Kernel Machines*. pp. 173–187. Lecture Notes in Computer Science, Springer, Berlin, Heidelberg (2003)
14. Meirovitch, Y., Mi, L., Saribekyan, H., Matveev, A., Rolnick, D., Shavit, N.: Cross-classification clustering: An efficient multi-object tracking technique for 3-d instance segmentation in connectomics. In: *Proceedings of the IEEE/CVF Conference on Computer Vision and Pattern Recognition (CVPR)* (June 2019)
15. Mnih, V., Badia, A.P., Mirza, M., Graves, A., Lillicrap, T., Harley, T., Silver, D., Kavukcuoglu, K.: Asynchronous methods for deep reinforcement learning. In: *International conference on machine learning*. pp. 1928–1937 (2016)
16. Mnih, V., Kavukcuoglu, K., Silver, D., Rusu, A.A., Veness, J., Bellemare, M.G., Graves, A., Riedmiller, M., Fidjeland, A.K., Ostrovski, G., et al.: Human-level control through deep reinforcement learning. *nature* **518**(7540), 529–533 (2015)
17. Quan, T.M., Hildebrand, D.G., Jeong, W.K.: Fusionnet: A deep fully residual convolutional neural network for image segmentation in connectomics. *arXiv preprint arXiv:1612.05360* (2016)
18. Song, G., Myeong, H., Mu Lee, K.: Seednet: Automatic seed generation with deep reinforcement learning for robust interactive segmentation. In: *Proceedings of the IEEE conference on computer vision and pattern recognition*. pp. 1760–1768 (2018)
19. Sutton, R.S., Barto, A.G.: *Reinforcement learning: An introduction*. MIT press (2018)
20. Uzkent, B., Ermon, S.: Learning when and where to zoom with deep reinforcement learning. In: *Proceedings of the IEEE/CVF Conference on Computer Vision and Pattern Recognition (CVPR)* (June 2020)